FINAL REPORT:
Sonar Detection of Buried Targets at Subcritical Grazing Angles: APL-UW Component

Kevin L. Williams, Eric I. Thorsos, Dajun Tang

DISTRIBUTION STATEMENT A
Approved for Public Release
Distribution Unlimited

Applied Physics Laboratory
College of Ocean and Fishery Sciences
University of Washington
Seattle, WA 98105-6698
phone: (206) 543-3949 fax: (206) 543-6785 email: williams@apl.washington.edu

Award Number: N00014-01-G-0460

LONG-TERM GOALS

Our long-term goal is to assist in developing robust techniques for the detection of buried mines at long ranges.

OBJECTIVES

The objective of the joint NSWC-PC/APL-UW project was to experimentally investigate subcritical buried target detection through rippled sediment/water interfaces.

The APL-UW portion of the joint project with NSWC-PC had two main components:

- Measurement of the ripple profile and small scale roughness for use in modeling the subcritical detections;
- Collaborate with NSWC-PC in carrying out Synthetic Aperture Sonar (SAS) experiments, in analysis of the acoustic data, and in the comparisons of the results to model predictions.

APPROACH

Measurements of subcritical buried target detections were made in controlled laboratory-type experiments at the NSWC-PC test pond. For these test pond measurements, a nearly 1-dimensional (1-D) ripple field was made with a machined rake[1]. This data were obtained on both spherical and cylindrical targets. Data from these targets were used for comparison with model predictions.

APL-UW supported the test pond effort by using the second generation seabed roughness measurement system known as the In-situ Measurement of Porosity 2 (IMP2) to measure seabed roughness along 4-meter tracks. This system gives an estimate of the ripple parameters and of

the small-scale 1-D roughness spectrum. For the efforts carried out as part of this work, orienting IMP2 relative to the ripples was essential. This orientation was carried out by divers.

An additional task included deployment of a new digital stereo camera system (first used in the Sediment Acoustics Experiment in 2004 – SAX04) in the Gulf in support of an AUV mine hunting exercise conducted by NSWC-PC in May 2006. As with IMP2, this system gives an estimate of the small-scale 1-D roughness spectrum but is less capable in determining the larger scale ripple parameters. It is, however, more portable and thus was the obvious choice for the vessel assets that were available.

WORK COMPLETED

Our efforts have focused on two separate tasks. The first benefited not only research under the present contract but also research being carried out in other work described in the "Related Projects" section. The second is unique to the current effort.

Task 1: SAS Signal-to-Noise Ratio (SNR) for buried spheres and cylinders

The detection of a deeply buried cylindrical object (buried to a depth of 50 cm) during a 1999 field experiment[2] continued to motivate our modeling and test pond experiments. In particular, our modeling efforts included the determination of the SAS SNR for a cylinder in the free field and for a buried cylinder in a subcritical geometry. The resulting sonar equation result was not obvious from the outset. This modeling result (along with the SAS SNR result for a sphere – which is more obvious) has been used, in conjunction with first order perturbation theory for subcritical penetration, in comparisons with data acquired on a buried sphere and cylinder.

Under separate funding we have developed a more sophisticated simulation capability that can simulate backscattering from the sediment interface, penetration due to ripples, and scattering from buried targets for specified geometries on a ping-by-ping basis. This model was compared to experimental data acquired in the test pond. We also used the NSWC-PC SWAT model to make similar predictions as well as another NSWC-PC model developed by Dr. Raymond Lim. The objective was to test the models experimentally and to check for consistency between models. Together the models represent a hierarchy of sophistication that can be applied to buried target detection depending on the needs of a particular program. For instance, a quick idea of the detectability of a buried object can be obtained using the sonar equation whereas a full ping-by-ping simulation may be desired as part of new system design.

Our previous work has led us to believe that subcritical penetration from a single component ripple field cannot explain the deep detection seen in 1999. This has led to an examination of subcritical penetration for more complex ripple structure. One such structure found in natural environments is the existence of a secondary ripple structure with a wavelength approximately half of the primary ripple. Thus pond experiments included subcritical penetration in the presence of a two-component ripple field.

Task 2: Deployment of stereo camera in Gulf of Mexico.

The APL digital stereo camera system was deployed at (30 02.190 N, 85 42.130 W) in April at what is designated as the Yankee site. At this site, three sets of stereo pairs were captured. These sets were each mosaicked to form a larger surface (approximately 60 x 40 cm). For each surface, the marginal spectra along the x and y directions were calculated and these spectra were fit by a power-law. These 1-D power-law fits were used to determine the 2-D power-law spectra needed for modeling.

RESULTS

Task 1: SAS Signal-to-Noise Ratio (SNR) for buried spheres and cylinders

As part of a basic research grant (see related projects section below) sonar equation level approximations were used to develop SAS SNR expressions for both spheres and cylinders. The result in dB for a sphere is (as one would anticipate):

$$SNR = 10\log(a^2/4) + 20\log(|f(ka)|) - SS - 10\log(A), \qquad (1)$$

where a is the radius of the sphere, k is the acoustic wavenumber, f is the form function[3] for the sphere, SS is the backscattering strength from the sediment/water interface and A is the area associated with the SAS areal resolution. This is a classical result, where the first two terms on the right side of Eq. 1 represent the target strength (TS) of the sphere, i.e., more generally, if the TS of the sphere is determined empirically or numerically (as done in the test pond work with fluid filled focusing spheres):

$$SNR = TS - SS - 10\log(A). \qquad (2)$$

This somewhat unremarkable result cannot be used in the case of cylinders, i.e., substitution of the classical TS for a cylinder into Eq. 2 will not give the correct SAS SNR. Detailed derivation instead gives, for a cylinder:

$$SNR = 10\log(aL_r/4\lambda) - SS - 10\log(\Delta r) \qquad (3)$$

where a is the cylinder radius, L_r is the length of the real horizontal apertures (assuming transmitter and receiver have the same horizontal aperture) used in the SAS system, λ is the acoustic wavelength and Δr is the range resolution (set by the bandwidth). This result has been tested successfully using numerical simulations where individual backscattered returns where calculated and then SAS processed.

To examine a buried object an additional factor must be added to account for the transmission of energy across the sediment/water interface twice, e.g., for a buried sphere:

$$SNR = 40\log(T) + 10\log(a^2/4) + 20\log(|f(ka)|) - SS - 10\log(A) \qquad (4)$$

where the transmission coefficient T for subcritical penetration via ripple scattering is calculated using first-order perturbation theory[4].

Figure 1 shows data and sonar equation model comparisons for the case of a sphere buried under a single component ripple. In addition, modeling results from a hierarchy of models with increased sophistication are also given in the figure. The results presented in Figure 1 indicate both consistencies between models and with the experimental data.

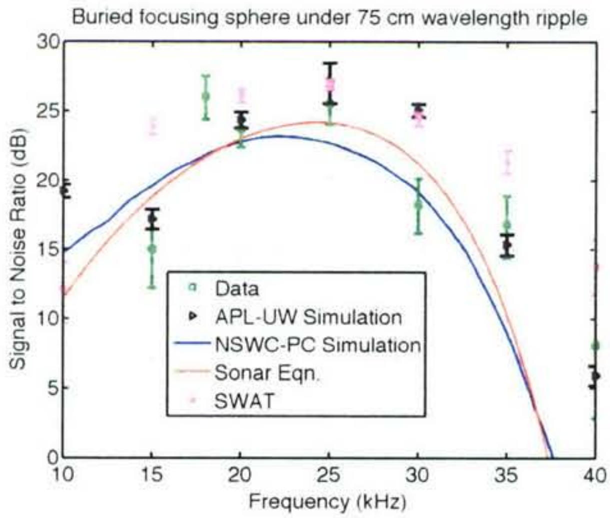

Figure 1. *Subcritical angle detection of a buried sphere. The data are from a NSWC-PC test pool experiment. The NSWC-PC simulation (blue curve) and sonar equation (red curve) assume plane wave incidence. The finite range to the target in the experiment allows more penetration than these plane wave models predict and is taken into account in the APL-UW simulation and in the Navy applied simulation code SWAT.*

In calculating T (Eq. 4) for the case of a two-component ripple field it is important to include the relative propagation phase of the contribution from each component. The two contributions add coherently and can result in enhancements of up to 12 dB in SNR over the SNR for each component separately. Figure 2 shows the model/data comparisons for the SAS SNR of a sphere and cylinder buried under a two-component ripple at a grazing angle of 20°.

The green and red circles are the data determined using two different regions of the bottom to determine the SNR. The blue curves represent the "eyeball" best fit to the data. The major factor in obtaining this best fit is the depth of burial to the top of the object. The interference of the two contributions to the backscattered signal (due to the two components of the ripple field) are extremely sensitive to this depth. Experimentally, the burial depth of each object was 10 cm with an estimated uncertainty of less than ± 3 cm. The blue curve for the sphere was determined using a burial depth of 8 cm. For comparison the dashed red curve in the sphere panel is the model result using a burial depth of 12 cm and the dashed green curve used 4 cm. The blue curve for the cylinder was determined using a burial depth of 12 cm. In that case the red dashed curve is for a burial depth of 16 cm and the dashed green curve used 8 cm.

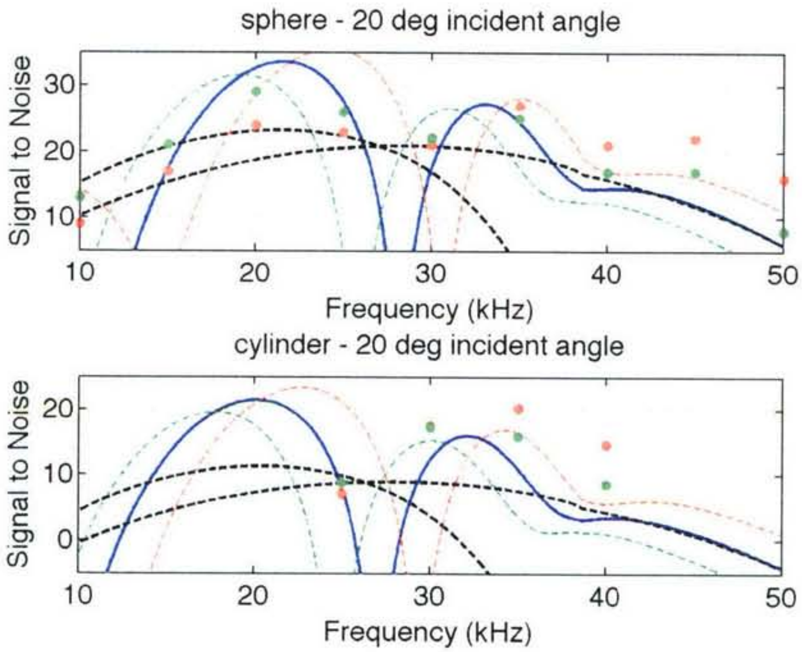

***Figure 2**. Model/data comparisons of the SNR in dB derived from SAS images of a sphere and a cylinder buried under a two-component ripple field. Note that the incident angles given in the figure are grazing angles.*

Finally, the dashed black curves in each panel are the SNR results if only one component of the ripple field were present. (It is important to note the enhanced SNR of the two-component result due to interference of the contribution from each component.) In carrying out the modeling a small scale roughness typical of what has been measured by IMP2 in previous pond work was used.

The comparisons in Fig. 2 give us confidence in our modeling capability. This model was then used in Fig. 3 to examine the SAS SNR for a cylinder buried 10 cm and 50 cm and a grazing angle of 10^{o}. All other parameters are as used in Fig. 2.

The salient points in Fig. 3 are that the interference of the contributions from the two components of the ripple field lead to much higher SNR at some frequencies than for each component separately and that, for the case shown here, one would predict that the deeply buried cylinder would be marginally detected in the 10-16 kHz band.

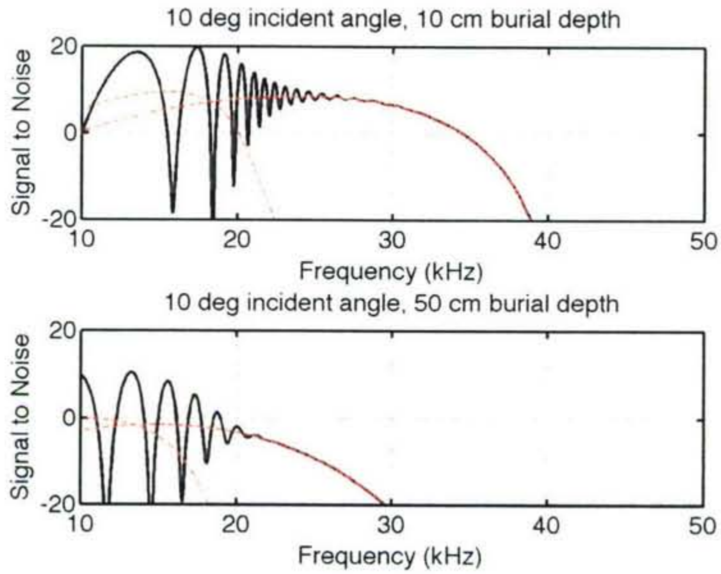

Figure 3. *SAS SNR in dB for a cylinder buried 10 cm and 50 cm under a two-component ripple field. Note that the incident angles given in the figure are grazing angles.*

Task 2: Deployment of stereo camera in Gulf of Mexico.

	Surface 1	***Surface 2***	***Surface 2***
Bearing of y-axis	17°	10°	348°
RMS Roughness	0.50 cm	0.47 cm	0.38 cm
W_2 (x)	0.00057 $cm^{4-\gamma_2}$	0.00061 $cm^{4-\gamma_2}$	0.00032 $cm^{4-\gamma_2}$
γ_2 (x)	3.21	3.25	3.39
W_2 (y)	0.00078 $cm^{4-\gamma_2}$	0.00048 $cm^{4-\gamma_2}$	0.00047 $cm^{4-\gamma_2}$
γ_2 (y)	3.26	3.20	3.72

All stereo camera images from the Yankee site detect the presence of an old ripple, $\lambda \approx 30$ cm. The spectral results for each stereo camera image are given in the table above. Mean values for 2-D power-law, derived from the table results are:

Spectral strength: $W_2 = 0.00054\ cm^{4-\gamma_2}$
Spectral exponent: $\gamma_2 = 3.34$

Figure 4 shows the stereo camera image, the marginal spectra and power-law fits for surface 1.

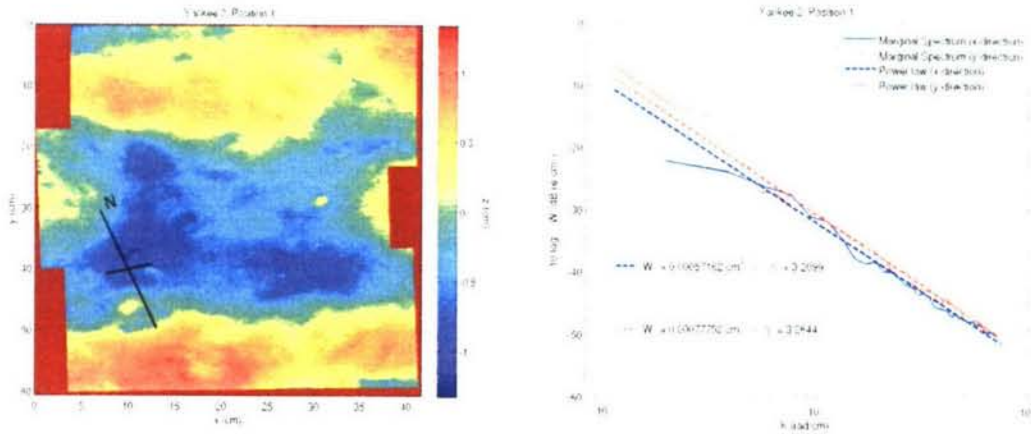

Figure 4. *Left side – topography image of sediment interface at Yankee site derived from digital stereo camera data. Right side – the marginal spectra and power-law fits derived from the topography data.*

IMPACT/APPLICATIONS

A demonstrated, quantitative understanding of the detectability of buried targets over a broad frequency range will allow development of sonar systems, software algorithms and operational concepts that incorporate environmental conditions in order to optimize detection and classification of buried mines.

RELATED PROJECTS

Title: High Frequency Sound Interaction in Ocean Sediments, Grant #: N00014-98-1-0040. This basic research grant supported an experiment in the fall of 2004 to examine basic sediment acoustics and deployment of a bottom-mounted SAS rail system to test our understanding of buried mine detection via sediment ripple. The website for the SAX04 experimental effort is: http://www.apl.washington.edu/projects/SAX04/summary.html .

REFERENCES

1. J. L. Lopes, C. L. Nesbitt, R. Lim, D. Tang, K. L. Williams, and E. I. Thorsos, "Shallow grazing angle sonar detection of targets buried under a rippled sand interface," *Proceedings of Oceans 2002*, Biloxi, MS, Oct 28-Nov 1, 2002.

2. J. E. Piper, K. W. Commander, E. I. Thorsos, and K. L. Williams, "Detection of Buried Targets Using a Synthetic Aperture Sonar," *IEEE J. Ocean. Eng.*, **27**, 495-504 (2002).

3. K. L. Williams, M. D. Richardson, K. B. Briggs, and D. R. Jackson, "Scattering of high-frequency energy from discrete scatterers on the seafloor: Glass spheres and shells," *Proceedings of the Institute of Acoustics* 23, 369-374 (2001).

4. D. R. Jackson, K. L. Williams, E. I. Thorsos, and S. G. Kargl, "High-frequency subcritical acoustic penetration into a sandy sediment," *IEEE J. Ocean. Eng.*, **27**, 346-361 (2002).

PUBLICATIONS

1. K. L. Williams, E. I. Thorsos, S. G. Kargl, D. Tang, J. L. Lopes and C. L. Dowdy, "Synthetic Aperture Sonar Measurements of Bistatic and Monostatic Scattering from Proud and Buried Targets (U)" (Secret), accepted in JUA(USN).